Journal of Applied Mechanics and Technical Physics, Vol. 36, No. 6, 1995

HYDRODYNAMICS AND DIFFUSION OF AN IMPURITY IN A CELL OF A TWO-PHASE MEDIUM*

P. K. Volkov and P. I. Geshev

UDC 532.529.6+533.15

In bubble towers, a two-phase mixture of a liquid with gas bubbles is formed when gas is forced through a perforated plate. The rate of ascent of the bubbles as a whole differs from the rate for a single bubble of the same dimensions, and the pattern of flow depends significantly on the distance between the bubbles. Theoretical and experimental study of the dynamic properties of the mixture poses formidable problems. Repeated attempts have been made to describe the two-phase mixture by isolating a certain cell of liquid containing a gas bubble or particle. The complexity of the problem has usually made it necessary to restrict the inquiry to a spherical cell, spherical bubbles, and nonseparated Stokes flow about the bubble. Conditions corresponding to triviality of the flow of mass, energy, and momentum have been imposed on the boundary of the cell. These conditions have then been used to determine the radius of the cell and the effective rate of bubble ascent [1]. Such an approach obviously does not take into account the actual interaction of the bubbles in the mixture, since they rise to the surface due to the flow of liquid behind the bubble – which means that mass flow takes place across the cell.

The main difficulty encountered in theoretical modeling entails selecting the geometry of the cell and formulating the boundary conditions on its external boundary so as to account for interactions between the bubbles and the carrying medium and between different bubbles. As a rule, the coalescence or fragmentation of bubbles is not considered.

Physical Formulation of the Problem. We will examine a mixture of a liquid with gas bubbles of one volume V located in layers. The distance between the layers is designated $2l$. The bubble dn in the layers is such that if a straight line is drawn vertically through the center of one of the bubbles, we obtain a chain of threaded bubbles. The bubbles are distributed uniformly within a given layer and form a hexagonal array in which each bubble is surrounded by six other bubbles of the same size. The distance between the centers gives us one more geometric parameters $2R_k$. In this case, it is natural to choose a right prism with a base in the form of a regular hexagon as the unit cell of the two-phase medium, i.e., a cell containing one bubble. The entire flow region is occupied by such cells. Thus, the geometric characteristics of a given cell are the height of the prism and the side of the base. This model gives a lower bound for the rate of bubble ascent, since if the bubbles were in any other position (slightly above or slightly below the layer) it would be easier for the liquid to blow downward through the bubble (which would also result in the bubble's rise).

Let us proceed to discussion of the boundary conditions on the external boundary of the cell. The characteristics should obviously be the same on the upper and lower bases of the prism, by virtue of the choice of cell. No flow occurs and no shear stresses are created through the lateral surface, i.e., this surface is the "free" surface. Thus, the entire flow field can be represented as a set of identical cells of liquid with a gas bubble inside. Of course, this situation is not actually realized, since a bubble increases in volume as it rises. However, the increase in bubble volume will be small for a system of bubbles of thickness h located far from the free surface, where the change in hydrostatic pressure is small compared to the pressure "at the level of the layer." The above is thus a good approximation. Liquid flows around the bubble in the coordinate system connected with the center of mass of the bubble, while the normal component of velocity is equal to zero on the lateral surface. The last condition is derived from the triviality of the shear stresses on the boundary of the cell. Now, the dynamics of the entire system of bubbles can be described by examining the problem of flow about a single bubble in a cell with the corresponding conditions of periodicity on the upper and lower bases and the conditions of nonflow and the absence of friction

*This study was made with financial support from the Russian Fund for Basic Research (Grant No. 95-01-99879a).

Translated from Prikladnaya Mekhanika i Tekhnicheskaya Fizika, Vol. 36, No. 6, pp. 68-76, November-December, 1995. Original article submitted December 16, 1994.

0021-8944/95/3606-0855$12.50

TABLE 1

l	Fr_{ch}	Fr_{ce}	$\overline{J}_{ch}$	$\overline{J}_{ce}$	Nu_{ch}/Nu_{ce}
3	4,83	0,53	18	29,3	1,068
			0,5+16,7+0,8	1,1+26,1+2,1	
6	4,0	0,5	18	28,2	1,076
			17,8+0,2	27,8+0,4	
9	3,37	0,45	19	28,3	1,08
			18,9+0,1	28,2+0,1	
20	2,73	0,43	20,3	29,8	1,08
				29,3+0,5	

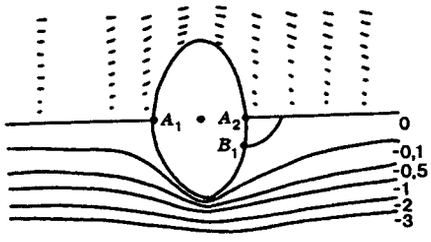

Fig. 1

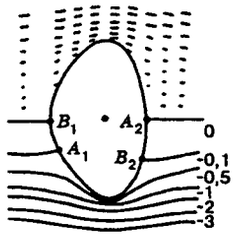

Fig. 2

on the lateral surface. This steady-state flow problem can be solved exactly. The degree to which its solutions agree with the solutions of the initial problem is determined by above propositions regarding the growth of bubbles as they rise.

Finally, we make one other assumption that reduces the problem to axisymmetric form. In numerical solutions, we will use a cylindrical cell with a base of radius R_k. It is difficult to evaluate the correctness of this proposition. In expressence, we are "transferring" boundary conditions from the lateral surface of a regular prism to the lateral surface of an inscribed cylinder. The movement of boundary conditions to a certain known line or surface is a technique that is often used to obtain different approximate models.

Mathematical Formulation of the Problem. We will use the Navier–Stokes equations as the mathematical model. These equations were written together with boundary conditions in [2] as they apply to the problem of flow about a gas cavity. Since the algorithm for solution of the problem is similar to that presented in [3] – where the procedure for realizing the periodicity conditions were described – here we write out only the boundary conditions for the lateral surface of the cell.

Written in terms of the stream function, the condition of nonflow gives this function a constant value. The exact value is determined on the basis of the following considerations: $\psi = 0$ in the coordinate system of the stationary liquid on the lateral surface, since there is not net flow through a section in which there are no bubbles. Translational motion of the liquid at the velocity U is superimposed on the flow field in the coordinate system of the bubble. In spherical coordinates (r, θ), this motion is described by the function $\psi = -Ur^2\sin^2\theta/2$. Since the equation of the surface $r = R_k/\sin\theta$, the stream function

$$\psi = -UR_k^2/2. \tag{1}$$

With allowance for (1), we can use the condition of triviality of the shear stresses to obtain a condition for the curl ω that coincides in form with the expression for ω on the free surface of the bubble [2]. Here, $R(\theta)$ represents the function for the lateral surface. Thus, "good" conditions that are easily realized within the framework of the algorithm [3] are obtained for the initial functions on the lateral surface of the cell. However, one other observation must also be made. Since the boundary of the cell has angles, the functions describing it in the spherical coordinate system will not be smooth: the first and second derivatives will have discontinuities at the points of inflections. This fact imposes additional restrictions on the computing procedure in connection with the deterioration in the accuracy of the finite-difference approximation of the Navier–Stokes equations, written in a curvilinear coordinate system.

The simplest method of avoiding these problems is to increase the number of theoretical points in the flow region. We used a uniform grid with 50 nodes for the angle θ and 61 nodes for the variable r. However, this proved inadequate for certain

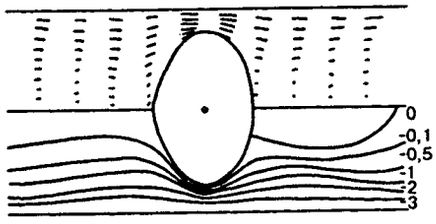

Fig. 3

cell geometries. The accuracy of the results was checked on the basis of test calculations performed with the use of intensive parameters and comparison of the results for flow past single bubbles and a chain of bubbles.

Analysis of Dimensionalities. As in [2-4], as dimensionless independent hydrodynamic parameters we used the Reynolds number Re = U2a/ν and Weber number We = $\rho U^2 2a/\sigma$, where $a = (3V/4\pi)^{1/3}$; ν, ρ, and σ are the kmn viscosity, density, and surface tension of the liquid. In our study, we add two more independent geometric parameters: l and R_k.

Let us examine the limiting cases of small and large R_k. When R_k is large, there is almost no interaction between the bubbles in the layer, i.e., we have one chain of identical bubbles. At small R_k, the hydrodynamics are completely determined by this interaction. In order to make a proper comparison (in addition to Re and We, the Froude number Fr = U^2/ga determines the character of the medium), we also present data for Re and We that correspond to the same values $M = \rho^3\nu^4 g/\sigma^3 = We^3/Re^4Fr$ and $R_\sigma = a/\delta_\sigma$, corresponding to a specific medium and specific bubble size a ($\delta_\sigma = (\sigma/\rho g)^{1/2}$ is the capillary constant) [4].

The drag coefficient C_d is usually defined as the ratio of the drag to the dynamic head. In the given case, since the drag is equal to buoyancy for steady ascent of the bubble, we have $C_d = \rho Vg/(1/2)\rho u^2 \pi a^2 = 8/3Fr$, and we find that determining Fr is equivalent to calculating C_d.

Results of Calculations. With assigned values of Re, We, l, and R_k, we use the algorithm in [3] to find the form of the bubble, the flow function ψ, ω, and the prm Fr. The latter conveys information on the rate of ascent of the bubble. Using the condition for the normal stresses, at We = 0 we have a spherical bubble with R $\equiv$ 2. The bubble changes form with an increase in We, but its volume V remains the same.

Table 1 shows calculated values of Fr for different l corresponding to a medium with M $\simeq$ 0.000002 and $R_\sigma \simeq 1$ ($a \simeq \delta_\sigma$). The second column corresponds to large R_k (a single chain of bubbles), while the third column shows data for the cell model with $R_k = 3$ (corresponding to dense packing of the bubbles in a layer in which the cross-sectional area of a bubble is more than 1/2 of the cross section of the cell, with allowance for its deformation).

Calculations for $l = 20$ (chain, Re = 100, We = 6.64) correspond to the case of a single bubble, when the effect of adjacent bubbles on its ascent is negligible. The values of Fr agree well with [3], which presented isolines of Fr. The comparison of Fr with calculations for a single bubble [4] fares somewhat more poorly. In the flow regime diagram, the corresponding point lies on the boundary of the vortex behind the bubble. Appearance of the vortex leads to oscillations of the surface and unsteady ascent of the bubble along a helix. As a result, the scatter of the experimental data is fairly significant in this region.

Flow about the single bubble is nonseparated and similar to the flow depicted in Fig. 1 (the solid lines are isolines of the stream function, while the dashes represent velocity vectors in different sections). Figure 1 shows the flow for $l = 6$ (Re = 100, We = 8.88). A small stagnation zone has already formed behind the bubble and its rate of ascent has increased. [At $l = 9$ (Re = 100, We = 7.68), the stagnation zone becomes even smaller, while there are no significant changes in the flow].

Figure 2 shows the flow for $l = 3$ (Re = 120, We = 10.5). The flow structure undergoes a qualitative change: although a stagnation zone forms between the bubbles near the axis of the chain, the rate of ascent (proportional to the root of Fr) increases by less than 10% compared to the case $l = 6$. The velocity profile in the different sections increases monotonically and fairly rapidly from a certain value on the bubble to unity.

Calculations performed for the cell model give values of Fr that are almost an order lower than for the chain. Thus, the rate of rise of the chain is nearly 2.5 times greater at $l = 20$ and three times greater at $l = 3$. Incidentally, the correctness of Fr can be checked here: the ratio of the values of Fr is equal to the ratio of the squares of the rates of ascent and – since the data corresponds to one medium and one bubble size – should be equal to the ratio of the squares of Re. In this case, the largest difference between the ratios is for $l = 6$ ($\sim$11%). The difference is smaller ($\sim$7%) for $l = 9$, and at $l = 3$ and 20

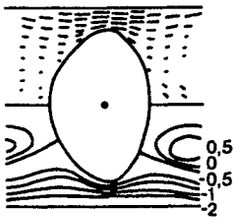

Fig. 4

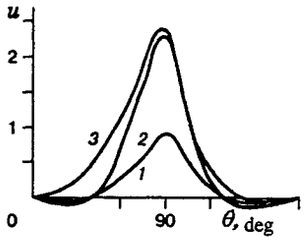

Fig. 5

they coincide. Considering that the tabular data corresponds to M = $2 \cdot 10^{-6}$ to within 5-7%, the results can be considered comparable.

A significant difference was also found in the patterns of flow. For example, at l = 20 (Re = 40, We = 1.1), there is a stagnation zone whose length is roughly equal to the diameter of a bubble. The flow structure in this case (and for l = 9) is the same as in Fig. 3, corresponding to l = 6 with the same Re and We. Comparison of the lengths of the velocity vectors for the chain of bubbles and in the cell shows a substantial increase in them between the bubbles in the layer. However, this difference is may be illusory, since the variables were converted to dimensionless form on the basis of the rate of ascent. In order to determine whether or not velocity actually increased, it is necessary to multiply the velocity values by the ratio of the rates of rise in the chain and the cell. Direct measurements and recalculation gives values that are approximately 10% less at the cell boundary between bubbles and significantly less with approach of the bases of the cell.

Figure 4 shows the flow pattern for l = 3 (Re = 40, We = 1.28). There is a fairly developed secondary flow between the bubbles. On the hole, the results follow the expected pattern and the rate of ascent turns out to be moderately dependent on the distance between the layers of bubbles – since the flow of the liquid is quite restricted. There is a simple explanation for the existence of a developed stagnation zone at the lower rate of rise (compared to the case of a chain of bubbles): in the case of the cell, there is considerably greater nonuniformity in liquid velocity around the bubble both in the region between the bubbles in the layer and along the bubbles' surfaces.

Figure 5 shows graphs of the velocity component tangent to the bubble u. Curves 1-3 correspond to Figs. 2, 4, and 3. The maximum value of u changes within a range of 10%. It ranges from 0.89 to 0.94 for a chain of bubbles and from 2.35 to 2.6 for a cell. Velocity is low near the frontal points. A decrease in l is accompanied by compression of the graph (curves 2 and 3 in Fig. 5) and the transition of the values to the negative region with the appearance of stagnation zones.

Diffusion of Gas from a Bubble to the Liquid. If we have the calculated field of the stream function, the form of the bubble, the structure of the flow field, and the separation point on the bubble, we can solve the problem of the diffusion of an impurity for a specified flow. The diffusion coefficients of molecules of gases dissolved in a liquid are very small. For the diffusion of molecules of oxygen in water, D ~ 10^{-9} m^2/sec. With an increase in the viscosity of the liquid, the diffusion coefficients decrease in inverse proportion to the viscosity coefficient and may be as much as 2-3 orders lower. This shows that the diffusion spectrallet number has very large values (Pe = Ud/D ~ 10^5-10^8, d = 2a). Thus, a thin diffusional boundary layer with a thickness on the order of δ_D ~ d/$\sqrt{Pe}$ is formed on the bubble surface. The concentration of dissolved gas in this layer C will change sharply from the equilibrium value on the bubble surface C_0 to the concentration of gas in the bulk liquid C_1.

The equation that describes diffusion in the boundary-layer approximation has the form

$$\frac{\partial C}{\partial t} + u\frac{\partial C}{\partial x} + v\frac{\partial C}{\partial y} = D\frac{\partial^2 C}{\partial y^2}, \tag{2}$$

while the boundary conditions are as follows:

$$C = C_0 \quad \text{at} \quad y = 0, \quad C \to C_1 \quad \text{at} \quad y \to \infty.$$

In Eq. (2), we introduced velocity u and the coordinate x along the free surface, as well as v andy perpendicular to this surface. The velocities v and u are connected by continuous equation, written in new coordinates:

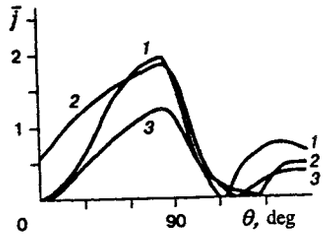

Fig. 6

$$\frac{\partial(Ru)}{\partial x} + \frac{\partial(Rv)}{\partial y} = 0$$

(R(x) is the distance from a point on the surface of the bubble to its axis of rotation). For v we have

$$v = -\frac{y}{R}\frac{\partial(Ru)}{\partial x}.$$

There is a self-similar solution for a wide range of diffusion problems with a free surface. This solution was used for wavy films in [5, 6] and for bubbles and droplets in [7, 8]:

$$\frac{C - C_0}{C_1 - C_0} = \frac{2}{\sqrt{\pi}}\int_0^{\eta} e^{-\eta^2} d\eta, \quad \eta = y/\delta(x,t).$$

Here, the thickness of the boundary layer δ satisfies the equation

$$(\delta^2)'_t + u(\delta^2)'_x + 2\frac{(uR)'_x}{R}\delta^2 = 4D \tag{3}$$

with the initial condition

$$\delta|_{t=0} = 0. \tag{4}$$

The complete solution of nonsteady problem (3)-(4) can be obtained by the method of characteristics [6]. In the present study, we performed detailed calculations only of the steady-state solution of Eq. (3). This solution is the intermediate asymptote and is valid for a certain time interval. For correct evaluation of this time interval, let us examine the structure of the solution of the complete problem in the neighborhood of two types of points:

a) with an incoming separating streamline (points A_1 and A_2 in Fig. 1); velocity u vanishes at A_1 and A_2 and the solution has the form

$$\delta^2 = \frac{2D}{\alpha}(1 - e^{-2\alpha t}), \tag{5}$$

where $\alpha = (uR)_x'/R \sim U/d$ is the rate of deformation of the liquid in the neighborhood of the inlet points. It can be seen from Eq. (5) that after the characteristic time $t_1 = d/U$ the thickness of the diffusion boundary layer becomes steady ($\delta \sim \sqrt{2Dd/U}$);

b) with an outgoing streamline (points B_1 and B_2 in Fig. 2); to evaluate the period of time required for the boundary layer to reach points on outgoing streamlines (type B), it is necessary to take into account the finite thickness of the diffusion boundary layer. This thickness is on the order of $\delta_D \sim d/\sqrt{Pe}$. Since the thickness δ_D is nontrivial, that part of the liquid saturated with gas that has diffused into it can overcome type-B points. In the neighborhood of the latter, surface velocity decays to zero in accordance with the law $u(x) \sim xU/d$. The below integral determines the time over which a liquid particle "floating" along the streamline and initially located the distance $\delta_D = d/\sqrt{Pe}$ from the free surface overcomes the neighborhood of point B with the dimension r_0

$$t_2 = \int_{r_0}^{\delta} \frac{dx}{u(x)} \sim \frac{d}{U}\ln(Pe).$$

After passing points of type B in times on the order of t_2, a liquid particle still requires the time $t_3 \sim l/U$ to travel the distance between the bubbles. Only after this will liquid particles with a high concentration of dissolved gases fall on the surface of the bubble. This will in turn produce a drop in the local and integral mass flows. Thus, the steady-state solution that is then calculated will be a certain intermediate asymptote that is valid for the time interval

$$d/U < t < \ln(\mathrm{Pe})\, d/U + l/U. \tag{6}$$

Since Pe is large, period of time (6) – corresponding to the occurrence of intermediate steady-state mass transfer – may turn out to be quite substantial.

Let us now proceed to the derivation of formulas for the steady-state solution. Equation (6) takes the form

$$(\delta^2)'_x + 2\frac{(uR)'_x}{uR}\delta^2 = \frac{4D}{u}. \tag{7}$$

The coordinate x will be reckoned from a point on the incoming streamline. Then the solution of (7) will be

$$\delta^2 = \exp\left(-2\int_0^x \frac{(uR)'_x}{uR}\,dx\right)\int_0^x \exp\left(2\int\frac{(uR)'_x}{uR}\,dx\right)\frac{4D}{u}\,dx = \frac{4D}{u(x)R(x)}\int_0^x R^2\,u\,dx. \tag{8}$$

Local mass flow is determined by the expression

$$j(x) = \frac{2D\Delta C}{\sqrt{\pi\delta(x)}}. \tag{9}$$

Total mass flow is obtained by integrating Eq. (9) over all sections between points of types A and B. The number of such sections may be one (when the flow is nonseparated), two (Figs. 1 and 3), or three (Figs. 2 and 4). Mass flow on an individual section of the free surface between points of types A and B is calculated in the form of an integral

$$J = \int_0^{x_B} j(x)\,2\pi\,R(x)\,dx = 4\sqrt{\pi D}\,\Delta C\Big(\int_0^{x_B} R^2 u\,dx\Big)^{1/2}. \tag{10}$$

The rate of diffusion flow is determined by the Nusselt number Nu and is calculated with allowance for the use of dimensionless variables by means of the formula

$$\mathrm{Nu} = J/2aD\Delta C = \sqrt{2aU/D}\;\bar{J} = \sqrt{\mathrm{Pe}}\;\bar{J}, \tag{11}$$

where $\bar{J}$ is the dimensionless mass flow.

Equation (11) provides little information itself, since the dimensionless parameter Pe contains a quantity U that is expressentially dependent on it. In this study, we are attempting to compare diffusion flows from a bubble of one size in a specified liquid for different geometric parameters of the problem. The natural characteristic for this is the ratio of the Nusselt numbers:

$$\mathrm{Nu}_{ch}/\mathrm{Nu}_{ce} = \sqrt{U_{ch}/U_{ce}}\;\bar{J}_{ch}/\bar{J}_{ce} = \sqrt[4]{\mathrm{Fr}_{ch}/\mathrm{Fr}_{ce}}\;\bar{J}_{ch}/\bar{J}_{ce}. \tag{12}$$

Equation (12) contains the ratio of the dimensionless diffusion fluxes $\bar{U}$ and the ratio of the hydrodynamic parameters Fr that are being determined. Now having calculated values of $\bar{J}$ and Fr, we can study the effect of the hydrodynamics of the flow on the rate of diffusion of gas from a bubble. Table 1 shows values of total diffusion flux and its terms on sections of the free surface for the above-solved hydrodynamic problems, as well as the ratio of Nusselt numbers for a bubble in a chain and in a cell.

The tabular results are rather surprising: for the same bubble volume (in the same liquid), the diffusion of gas from the bubble into the liquid is nearly independent of the distance l. The explanation for this lies in the structure of the diffusion

flow: the largest contribution is made by the region of the equator of the bubble, where tangential velocity u has a maximum (Fig. 5).

Figure 6 presents graphs of the function of local diffusion flux $\bar{j}(\theta)$. Curves 1-3 correspond to Figs. 4, 3, and 2. The correlation between $u(\theta)$ and $\bar{j}(\theta)$ is clear. The value of $\bar{j}(\theta)$ on the front part of the bubble (where the liquid flows to the bubble surface) is greater than on the rear part (where the liquid stagnates) except for the neighborhood of the rear point – where there is a separation zone.

Even more surprising is the data in the last column of Table 1. The ratio of the diffusion fluxes for the bubbles in a chain and in a cell is roughly constant. Total flux is 7-8% greater in the case of the chain than in the case of the cell. Considering the accuracy of calculation of Fr, the tabular data, and the accuracy of calculation of $\bar{J}$ on the basis of (10), we can conclude that the diffusion fluxes are nearly equal, rather than one type of flow having an advantage. It follows in turn from this conclusion that diffusion will be most intensive in a certain volume of liquid when the largest number of bubbles of a specified size ascend through a layer of liquid of thickness h during the period of time Δt. This second conclusion is valid not only for short time intervals Δt for which the steady-state solution obtained from (6) is valid, but also for times long enough for the beginning of unsteady interaction of the diffusion boundary layers of adjacent bubbles.

Conclusions. The numerical solutions obtained from the cell model agree well with previous calculations from modeling of the surfacing of chains of bubbles and single bubbles. This means that, on the whole, the periodicity conditions and the conditions on the external boundary of the cell adequately reflect the actual interaction of bubbles in a gas–liquid medium. The problem examined here is similar to the case of the surfacing of a bubble in a pipe with a quiescent liquid [9]. The difference is that the condition of adhesion to the pipe wall, slowing the liquid to zero velocity, was imposed in [9]. In this investigation, we assumed that there was no friction at boundary of the cell. Thus, while the liquid in [9] flowed past the bubble in a stream located near the bubble, in our study the stream was near the wall of the cell.

The results of a series of calculations performed for bubbles of the same size in liquid with $M \simeq 2 \cdot 10^{-6}$ show that the diffusion of gas in liquid should be intensified by changing the size of the bubbles in the two-phase medium. There are grounds for believing that the conclusions reached here will also hold for media with other M. In fact, there should not be any significant changes in the system if the driving force (buoyancy) remains constant and if the shear stresses at the boundaries are equal to zero or if the periodicity conditions are satisfied. The situation may change if thermocapillary or concentration-capillary forces on the surface of the bubbles turn out to be dominant.

The conclusions stated in the previous paragraph are also valid for the propagation of heat, which is also described by an equation of type (2) with a solution of type (8), (10). However, the use of this solution requires very large thermal spectrallet numbers.

REFERENCES

1. I. O. Protod'yakonov and I. E. Lyublinskaya, Hydrodynamics and Mass Transfer in Gas–Liquid Systems [in Russian], Nauka, Leningrad (1990).
2. C. I. Christov and P. K. Volkov, "Numerical investigation of the steady viscous flow past a stationary deformable bubble," J. Fluid Mech., **158**, 341-364 (1985).
3. P. K. Volkov, "Motion of a chain of bubbles in a vertical channel with a viscous liquid," Prikl. Mekh. Tekh. Fiz., No. 3, 87-91 (1991).
4. P. K. Volkov, "Hydrodynamics of surfacing bubbles and droplets," Fiz. Inzh. Zh., **66**, No. 1, 93-123 (1994).
5. E. Ruckenstein and C. Berbente, "Mass transfer to falling liquid film at low Reynolds numbers," Int. J. Heat Mass Transfer, **11**, No. 4, 743-753 (1968).
6. P. I. Geshev and A. M. Lapin, "Diffusion of a weakly dissolved gas in falling wavy liquid films," Prikl. Mekh. Tekh. Fiz., No. 6, 106-112 (1983).
7. B. T. Chao, "Transient mass and heat transfer to translating droplet," J. Heat Transfer, **91**, No. 2, 273-281 (1969).
8. Yu. P. Gupalo, A. D. Polyanin, and Yu. S. Ryazantsev, Mass and Heat Transfer of Reacting Particles and a Flow [in Russian], Nauka, Moscow (1985).
9. P. K. Volkov, "Surfacing of a gas bubble in a pipe filled with a viscous liquid," Prikl. Mekh. Tekh. Fiz., No. 6, 98-105 (1989).